

Supporting Information

Solution-processed UV Light Emitting Diode Based on Butyltriphenylsilane Modified Phenanthro[9, 10-*d*] imidazole with High Efficiency

Zhao Gao,^{a,c} Fangming Liu,^a Jinyu Li,^a Gang Cheng,^{b,*} and Ping Lu^{a,*}

Contents

1. Experimental Section.....	2
2. Synthesis and Characterization.....	2
Scheme S1 Molecular structures of PPI and SiBPI.....	3
Fig. S1 ¹ H NMR spectra of SiBPI.....	3
Fig. S2 FTIR spectra of SiBPI.....	3
3. Thermal properties.....	3
Fig. S3 The DSC graph of SiBPI (recorded at a heating rate of 10 K min ⁻¹ under a nitrogen flow).4	
4. Electroluminescence devices.....	4
Fig. S4 (a) The EQE for the vacuum deposition device A; Insert: EL emission of SiBPI at 5 V; (b) The current efficiency versus voltage for device A; Insert: CIE coordinates of SiBPI at 5 V.....	5
Fig. S5 The EL emission of SiBPI from 5 V to 10 V for vacuum deposition device A.....	5
Fig. S6 The current efficiency and luminance versus voltage of SiBPI for vacuum deposition device A.....	6
Fig. S7 The current efficiency and power efficiency versus voltage of SiBPI for solution-processed device B.....	6
Fig. S8 The luminance and current density versus voltage of SiBPI for solution-processed device B.....	7
Fig. S9 The EL emission of SiBPI from 6 V to 11 V for solution-processed device. Insert: CIE coordinates at 6 V.....	7

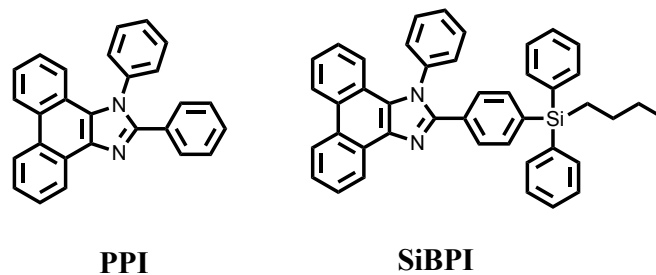
1. Experimental Section

All the reagents and solvents used for the syntheses were purchased from Aldrich or Acros and used as received. All reactions were performed under a dry nitrogen atmosphere. The NMR spectra were recorded on AVANCZ 500 spectrometers at 298 K by utilizing deuterated chloroform (CDCl_3) or dimethyl sulfoxide (DMSO) as solvents and tetramethylsilane (TMS) as internal standard. The elemental analysis were performed by a Flash EA 1112, CHNS-O elemental analysis instrument. The MALDI-TOF-MS mass spectra were recorded using an AXIMA-CFRTM plus instrument. UV-vis absorption spectra were recorded on a UV-3100 spectrophotometer. Fluorescence measurements were carried out with a RF-5301PC. The differential scanning calorimetry (DSC) analysis was determined using a NETZSCH (DSC-204) instrument at $10\text{ }^\circ\text{C min}^{-1}$ under nitrogen flushing. Cyclic voltammetry (CV) was performed with a BAS 100W Bioanalytical Systems, using a glass carbon disk ($\Phi = 3\text{ mm}$) as the working electrode, a platinum wire as the auxiliary electrode with a porous ceramic wick, and Ag/Ag^+ as the reference electrode standardized by the redox couple ferricinium/ferrocene. All solutions were purged with a nitrogen stream for 10 min before measurement. The procedure was performed at room temperature and a nitrogen atmosphere was maintained over the solution during measurements.

Device fabrication

The EL devices were fabricated by vacuum deposition of the materials at 10^{-6} Torr onto ITO glass with a sheet resistance of $25\ \Omega\ \text{square}^{-1}$. All of the organic layers were deposited at a rate of $1.0\ \text{Å s}^{-1}$. The cathode was deposited with LiF (1 nm) at a deposition rate of $0.1\ \text{Å s}^{-1}$ and then capping with Al metal (100 nm) through thermal evaporation at a rate of $4.0\ \text{Å s}^{-1}$. The electroluminescence (EL) spectra and CIE coordination of these devices were measured by a PR650 spectra scan spectrometer. The luminance-current and density-voltage characteristics were recorded simultaneously with the measurement of the EL spectra by combining the spectrometer with a Keithley model 2400 programmable voltage-current source. All measurements were carried out at room temperature under ambient conditions.

2. Synthesis and Characterization



Scheme S1 Molecular structures of PPI and SiBPI.

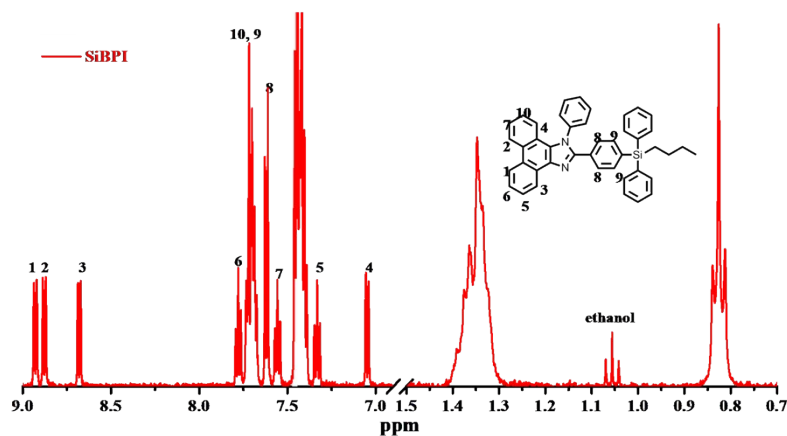


Fig. S1 ¹H NMR spectra of SiBPI.

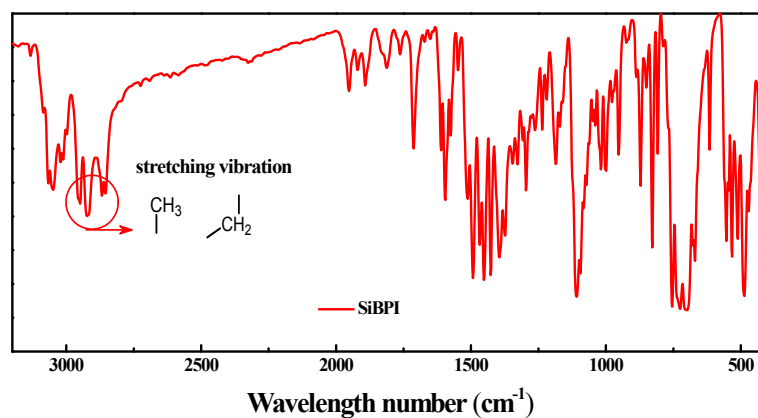


Fig. S2 FTIR spectra of SiBPI.

3. Thermal properties

The thermal property of SiBPI is investigated using differential scanning calorimetric (DSC) by three heating cycle upon 400 °C. The T_m of SiBPI was measured to be at 190 °C by first heating. In second and third heating cycle, the T_g of SiBPI was obtained at 75 °C. However, upon further heating beyond T_g , no exothermal peak of melting temperature was observed in second and third heating cycle.

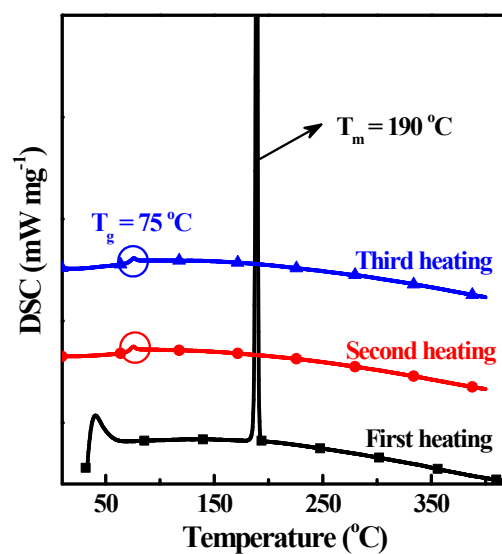


Fig. S3 The DSC graph of SiBPI (recorded at a heating rate of 10 K min^{-1} under a nitrogen flow).

4. Electroluminescence devices

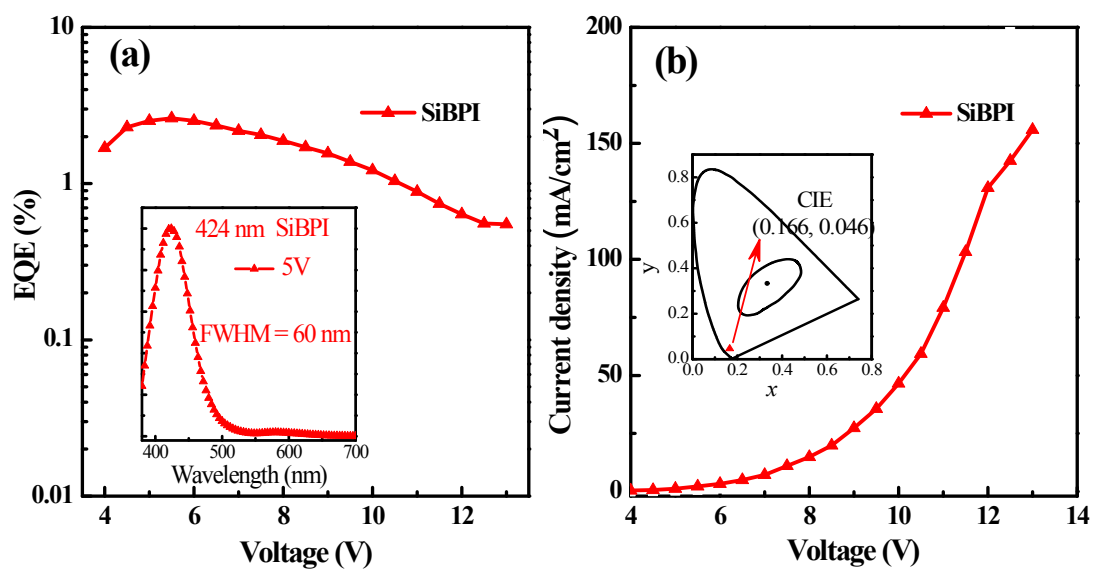


Fig. S4 (a) The EQE for the vacuum deposition device A; Insert: EL emission of SiBPI at 5 V; (b) The current efficiency versus voltage for device A; Insert: CIE coordinates of SiBPI at 5 V.

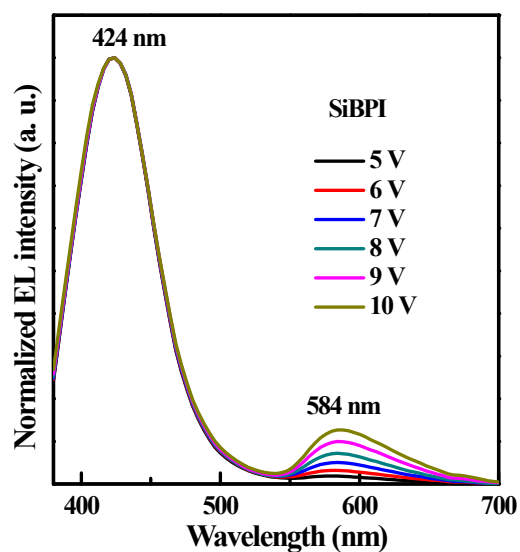


Fig. S5 The EL emission of SiBPI from 5 V to 10 V for vacuum deposition device A.

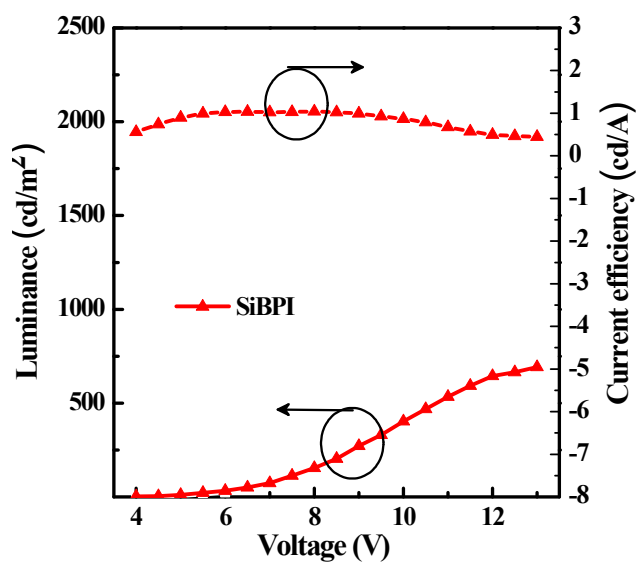


Fig. S6 The current efficiency and luminance versus voltage of SiBPI for vacuum deposition device A.

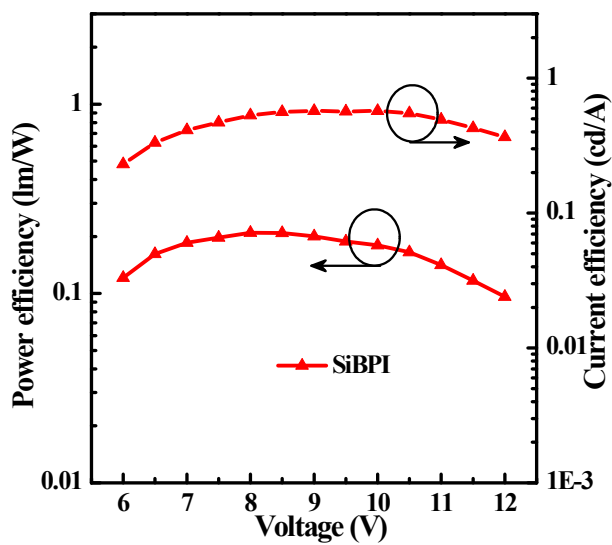


Fig. S7 The current efficiency and power efficiency versus voltage of SiBPI for solution-processed device B.

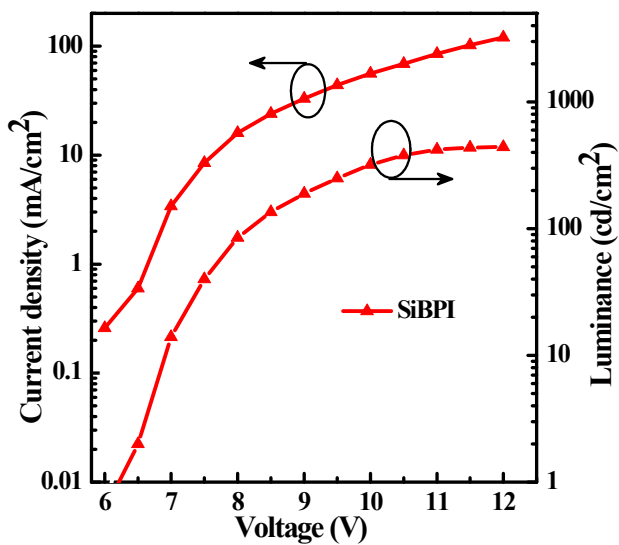


Fig. S8 The luminance and current density versus voltage of SiBPI for solution-processed device B.

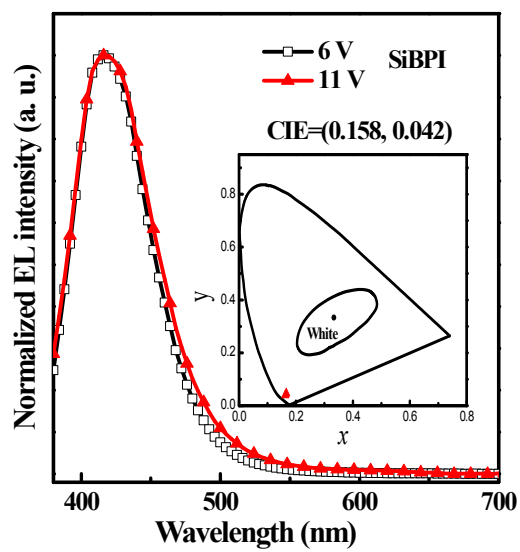


Fig. S9 The EL emission of SiBPI from 6 V to 11 V for solution-processed device. Insert: CIE coordinates at 6 V.